

11 JUN 1948

UNCLASSIFIED

NACA

## RESEARCH MEMORANDUM

INVESTIGATION AT SUPERSONIC SPEED ( $M = 1.53$ ) OF THE PRESSURE  
DISTRIBUTION OVER A  $63^\circ$  SWEEP AIRFOIL OF  
BICONVEX SECTION AT ZERO LIFT

By Charles W. Frick and John W. Boyd

Ames Aeronautical Laboratory  
Moffett Field, Calif.

CLASSIFICATION CANCELLED

CLASSIFIED DOCUMENT

Authority *ACAR 92378* Date *2/18/54*By *Ymt 9/2/54* See

This document contains classified information affecting the National Defense of the United States within the meaning of the Espionage Act, USC 5012 and 5013. Its transmission or the revelation of its contents in any manner to an unauthorized person is prohibited by law. Information so classified may be imparted only to persons in the military and naval establishments of the United States, appropriate civilian officers and employees of the Federal Government who have a legitimate interest therein, and to United States citizens of known loyalty and discretion who of necessity must be informed thereof.

NATIONAL ADVISORY COMMITTEE  
FOR AERONAUTICS

WASHINGTON  
June 10, 1948

UNCLASSIFIED

NACA LIBRARY  
LANGLEY MEMORIAL AERONAUTICAL  
LABORATORY  
Langley Field, Va.

UNCLASSIFIED

## NATIONAL ADVISORY COMMITTEE FOR AERONAUTICS

RESEARCH MEMORANDUMINVESTIGATION AT SUPRESONIC SPEED ( $M = 1.53$ ) OF THE PRESSURE  
DISTRIBUTION OVER A  $63^\circ$  SWEEP AIRFOIL OF  
BICONVEX SECTION AT ZERO LIFT

By Charles W. Frick and John W. Boyd

## SUMMARY

The results of an investigation at supersonic speed of the distribution of pressure at zero lift over the surface of a swept airfoil of biconvex section are presented. The airfoil used for the experiment was composed of sections 7 percent thick in streamwise planes and was swept back  $63^\circ$ . The aspect ratio was 1.66 and the taper ratio 1. The tests were made at a Mach number of 1.53 over a Reynolds number range of  $0.481 \times 10^6$  to  $3.25 \times 10^6$ .

The measured pressures have been compared with theoretical values calculated from thin-airfoil theory. In general, good agreement is found except where the limitations of the linear theory may be expected to manifest themselves: namely,

1. The region of influence of the subsonic trailing edge on the pressure distribution, which determines the location of the pressure minimum, does not extend up to the Mach line from the root trailing edge as theory predicts, since the local Mach numbers on the airfoil are appreciably greater than that of the stream. The position of the pressure minimum is therefore moved rearward.

2. The pressure recovery behind the pressure minimum is greater than predicted by theory and, although the data are not conclusive, appears to take place, in part, through a shock wave.

These deviations from the linear theory result in an appreciable increase in the pressure drag over that calculated by theory.

UNCLASSIFIED

### INTRODUCTION

The adaptation of the theory of sound waves of small amplitude to the aerodynamics of bodies moving at supersonic speeds has been found to be very fruitful in producing methods of calculating pressure distributions for thin wings at zero lift (references 1, 2, and 3). These methods are limited, however, to wings which are thin in both longitudinal and transverse sections, so that

1. The axial perturbation velocities are small with respect to the absolute value of the difference between the stream velocity and the velocity of sound in the fluid.

2. The lateral perturbation velocities are small both with respect to the stream velocity and the velocity of sound in the fluid.

The theory, of course, assumes that the fluid is inviscid. This assumption has been found to give satisfactory results in the theoretical calculations of pressure distributions at subcritical speeds for flows not involving separation, the effect of viscosity being confined primarily to a thin layer of fluid next to the airfoil surface. The range of applicability of the perfect fluid theory at supersonic speeds must be determined by careful experiment. Experiment must also be relied on to show how well the linearized theory predicts the pressure-distribution characteristics of wings, the sections of which cannot be said to be thin.

Agreement between theory and experiment has been found to be good for unswept airfoils, at least for the portion of the span unaffected by flow near the tips. The results of an investigation for a swept-back airfoil at zero lift, which may be treated theoretically by references 2 and 3, are discussed in the present report. The material for this report was obtained as a part of an investigation of the pressure-distribution characteristics of swept airfoils at supersonic speeds both at zero lift and at angles of attack.

### SYMBOLS

$x, y$	cartesian coordinates
$M$	local Mach number on airfoil surface
$Re$	Reynolds number based on the streamwise chord of 6 inches

$q_o$	dynamic pressure $\left(\frac{1}{2}\rho_o V_o^2\right)$
$\rho_o$	density of stream
$V_o$	free-stream velocity
$\frac{p_o - p_w}{q_o}$	stream static pressure coefficient
$p_o$	stream static pressure
$p_w$	reference static pressure
$P$	pressure coefficient $\left(\frac{p - p_o}{q_o}\right)$
$p$	local static pressure on airfoil
$c_d$	section pressure drag coefficient

#### DESCRIPTION OF APPARATUS

##### Wind Tunnel

The experimental investigation discussed herein was made in the Ames 1- by 3-foot supersonic wind tunnel No. 1. This wind tunnel is of the closed-return variable-pressure type operated at present with a nozzle of fixed dimensions which gives a Mach number of 1.53 in a 1- by 2-1/2-foot test section. It is fully described in reference 4.

##### Model and Model Support

Because of considerations of desirable test Reynolds numbers and model structural design and since it was not necessary to measure forces or moments with a balance system, a semispan model was selected, mounted as shown in figures 1 and 2. In order to avoid the undesirable effects of the tunnel-wall boundary layer, the model was supported on a thin circular plate positioned in the stream in a vertical plane 1-1/4 inches from the tunnel side wall so as to bypass the tunnel-wall boundary layer (fig. 2). This plate was, in turn, mounted on a steel plate placed in the frame of the window in the tunnel wall ordinarily used for viewing the flow around models with the schlieren apparatus.

In order to avoid choking of the flow in the boundary-layer bypass channel, the channel was expanded in the downstream direction by

machining the steel plate which replaced the window as shown in figure 2.

Disturbances in the tunnel air stream due to the model-support system may originate from the following sources:

1. The outer surface of the model-support plate
2. The supersonic edge of the model-support plate
3. The boundary-layer bypass channel around the subsonic edges of the model-support plate

In order to minimize the disturbances, the following precautions were taken:

1. The surface of the model-support plate was machined flat to a tolerance of  $\pm 0.002$  inch.
2. The edge of the model-support plate was beveled to a sharp knife edge, the bevel located on the side of the plate next to the tunnel wall. In this way, the side of the plate on which the model was mounted was flat and parallel to the stream, resulting in a minimum disturbance, and the shock wave due to the finite thickness of the plate was diverted behind the plate into the boundary-layer bypass channel.
3. The model was so located on the support plate that the entire span, except for a small portion of the tip, was outside the zone of influence of disturbances propagated from the bypass channel around the subsonic edge of the support plate.

The model selected for the investigation was composed of constant-chord biconvex circular-arc sections in planes perpendicular to the leading edge which was swept  $63^{\circ} 45'$ . Circular-arc sections were chosen for two reasons: First, because the theoretical method of reference 2 for calculating pressure distributions is restricted at present to airfoils with sharp leading edges; and, second, because the construction of the model is much simplified. The airfoil sections in planes parallel to the stream, therefore, consisted of elliptical arcs. The thickness of the sections in planes parallel to the stream was chosen as 7 percent of the chord primarily from considerations of model strength. A sketch of the model giving pertinent dimensions is shown in figure 3.

A chord of 6 inches, constant across the span, was selected to obtain desirable test Reynolds numbers and to provide sufficient size for the difficult task of placing pressure orifices without undue sacrifice in model span and aspect ratio. A maximum span of 5 inches for the airfoil was dictated by consideration of the reflection from the opposite tunnel wall of the shock wave originating at the apex of the airfoil. At the test Mach number of 1.53, the trailing edge of the tip lies about 1 inch ahead of this reflected wave. The resulting aspect ratio was 1.66. The tip of the airfoil, cut off parallel to the stream, was formed by simply rotating the tip section about its chord line.

The model was fitted with 74 pressure orifices 0.013 of an inch in diameter arranged to measure the chordwise distribution of pressure for sections parallel to the air stream at five spanwise positions as shown in figure 3. Stainless-steel tubes were connected to these orifices and conducted spanwise through a channel in the airfoil to the root and out of the tunnel through the model support. The orifice pressures were measured on a multiple-tube manometer using as a liquid an organic compound, tetrabromoethane, which has a specific gravity of 2.96 at a temperature of 70° F. All pressures, including the test-section reference pressure and the total head of the air stream, were recorded photographically.

## ANALYSIS OF DATA

### Air-Stream Characteristics

Prior to actual tests of the airfoil, an investigation of the wind-tunnel air stream was made to determine the character of the flow as influenced by the model support system. Surveys of the static pressure of the stream were made parallel to the axis of the tunnel at three positions across the stream in the horizontal plane in which the model was placed.

These surveys were made with a static pressure probe consisting of a 100-caliber ogival needle, 0.10 inch in diameter. Pressure orifices were placed in the needle at a position for which an analysis using linear theory indicated that the local pressure was equal to that of the stream.

The results of the surveys are given in figure 4. The Reynolds numbers indicated in these figures are based on the 6-inch chord of the wing at tunnel total pressures of 3, 12, and 24 pounds per square inch, respectively. The data are given as the difference between the



pressure measured with the needle and the pressure measured by the test-section reference static-pressure orifice in terms of the dynamic pressure of the stream. This reference pressure orifice is located on the side wall of the tunnel 3.06 inches ahead of the apex of the leading edge of the model airfoil. The pressure coefficients obtained are plotted as a function of the distance downstream from the location of the test-section static-pressure orifice. The location of the wing section at the survey station is shown in each figure.

Examination of these data and comparison with previous surveys of the stream along the center line without the boundary-layer plate show that practically the only effect of the model-support system was the propagation of a weak compression wave in the stream which can be traced to the leading edge of the model-support plate. This wave, which appears on the pressure survey of figure 4(a) 4 inches downstream of the position of the test-section reference-pressure orifice, becomes of negligible magnitude at appreciable distances outboard of the support plate. (See figs. 4(b) and 4(c).)

At first, the compression wave was believed to be due to the fact that the flat outer side of the support plate was not alined with the stream, but further tests, with the incidence of the plate varied, showed merely a change in the general pressure level. It seems probable that this disturbance results because it is impossible to produce a leading edge sharp enough in terms of molecular dimensions to prevent the formation of a detached wave which is propagated out into the stream, even though the flat side of the plate is alined with the stream. Also, the formation of a boundary layer on the plate probably makes the edge of the plate effectively blunt.

The existence of this disturbance had little effect on the pressures in the stream over the region in which the wing was placed. The pressure variation over this region is within  $\pm 1/2$  percent of the average dynamic pressure of the stream. The exact correction for the static-pressure variation in the stream is exceedingly complex, requiring a knowledge of the source of the pressure disturbances and the manner in which they are reflected by the model. For the present report, corrections to the measured pressure data were made by subtracting from the reading of each orifice the difference in static-pressure coefficient between the value at the position of the orifice and the average value over the region of the wing. This amounts to an approximate correction, the precision of which will be discussed later.

### Reduction of Data

As mentioned previously, the pressures were recorded by photographing the manometer board. The data were then plotted directly in pressure-coefficient form through the use of a film reader. This device, in essence, consists of a ground-glass screen on which is projected an image of the photographic negative. The magnification of the image can be controlled to such an extent that the height of a liquid column on the negative representing the dynamic pressure may be adjusted to equal the dimension on transparent cross-section plotting paper equivalent to a unit of dynamic pressure. The readings of all the pressure orifices may then be plotted directly as pressure coefficients. The correction for the static-pressure variation in the stream, discussed previously, was made subsequent to plotting.

The pressure drag of the airfoil at the various stations, for which the pressure distributions were measured, was calculated by plotting the product of the reading of each pressure orifice and the local airfoil slope as a function of the chordwise dimension and integrating mechanically. Since the local slope is known accurately, reasonable accuracy is obtained.

### Precision

Since the flow in the wind tunnel is free of strong shock waves, there are five items in which inaccuracies may occur in determining experimentally the pressure-distribution characteristics of an airfoil:

1. Possible error of the pressure probe
2. The error involved in using a superposition process to account for the variation in the stream static pressure over the region of the wing
3. The error involved in reducing the data with a film reader
4. Errors of the individual wing pressure orifice
5. The errors introduced by variations in stream angle

No means for determining the inaccuracy of the pressure probe is available at present. It is estimated, however, from calculation of the pressure distribution over the probe and from what is known about

the inaccuracies of pressure orifices, that the pressure probe measures the local stream static pressure within  $\pm 1/2$  of 1 percent. This is the accuracy of the dynamic pressure used in obtaining pressure coefficients.

The correction made for the pressure variation in the stream over the region of the wing discussed previously is an approximate correction. The true correction, which is very complex, may be as much as twice as large under certain conditions. In general, the superpositions used should be about 75 percent correct. Since the static pressure variation in the stream over the wing is between  $\pm 1-1/2$  and 2 percent of the stream dynamic pressure, the accuracy of the correction should give true pressure coefficients within  $\pm 1/2$  of 1 percent of the dynamic pressure.

The use of a film reader in plotting pressure coefficients involves an error of about  $\pm 1/3$  of 1 percent at the highest wind-tunnel pressures where most of the pressure measurements were made.

Examination of the data obtained from test of the airfoil shows that orifices at the same chordwise and spanwise positions on the upper and lower surfaces of the wing read the same pressure within  $\pm 1/2$  of 1 percent of the stream dynamic pressure, which is remarkable in view of the difference in contour that may result from the machining process. As a conservative measure, this error may be taken as the orifice error.

Surveys of the wind-tunnel stream show small stream angles existing over the region in which the wing was placed. It is evident from a study of the pressure data obtained for the airfoil, however, that their influence was negligible, since the lift due to the induced camber effect that should appear does not exist.

The final accuracy of the pressure-distribution data can be obtained by taking the square root of the sum of the squares of the various inaccuracies. The final pressure coefficients are found to be true values within  $\pm 1$  percent of the dynamic pressure or within 5 percent of the maximum perturbation pressure.

#### THEORY

In reference 2, R. T. Jones has shown that through the use of oblique transformations it is possible to arrive at solutions for the pressure-distribution characteristics of swept airfoils at zero lift. While the method presented is applicable to airfoils of more

[REDACTED]

or less arbitrary section, provided the leading edge is sharp, calculation of any but wedge, diamond, or parabolic arc airfoils is complex. In general, the approximation involved in assuming the solution for airfoils composed of elliptical or circular arcs to be the same as for a parabolic-arc airfoil is very good if the thickness of the airfoil is small. For the airfoil of the present investigation, which is composed of elliptic-arc sections in the streamwise direction, however, the thickness is sufficiently large as to require a somewhat closer approximation made by increasing the strength of the line sources at the leading and trailing edge to give the true wedge angles. The theoretical pressure distributions computed in this manner are compared with the experimental results in the following section.

## RESULTS AND DISCUSSION

### Pressure Distribution

Pressure-distribution measurements were made for a range of Reynolds number of  $0.481 \times 10^6$  to  $3.25 \times 10^6$  by varying the total pressure of the wind tunnel from 3 pounds per square inch to 24 pounds per square inch absolute. The results of these tests are given in figure 5 for the various spanwise stations at which the chordwise variation of the pressure was obtained.

The agreement between the linear theory of reference 2 and experiment, as indicated by the data of this figure, is seen to be reasonably good with the following exceptions:

1. At the lowest Reynolds number  $0.481 \times 10^6$ , the results indicate that laminar separation occurs, since the experimental pressure distributions show no recovery of pressure over the rear portion of the airfoil.
2. At the higher Reynolds numbers, laminar separation does not occur and the agreement between theory and experiment is good except within the zone of action of the subsonic trailing edge.

The occurrence of laminar separation at the lowest Reynolds number is in agreement with the results of previous investigations in this Reynolds number range. Visual observations of the pressure-measuring manometers during the tests showed that laminar separation existed on the airfoil at Reynolds numbers of  $1 \times 10^6$  or less. As this value was exceeded, the character of the flow over the rear portion of the airfoil changed abruptly, showing a marked increase in pressure and

indicating that the boundary-layer flow had become turbulent, enabling the flow to cling to the surface.

At the higher Reynolds numbers, where laminar separation does not occur, the agreement between theoretical and experimental pressure distributions is poor over the portion of the airfoil which lies within the Mach cone of the trailing edge. The region influenced by the subsonic trailing edge is found, from the experimental pressure distributions, to be smaller than given by the linear theory. This difference results from the fact that, in the linear theory, pressure disturbances are propagated along Mach lines. In actuality, since the local Mach numbers over the airfoil are appreciably different from that of the stream, weak pressure disturbances are propagated along curved lines, which may be defined as having such curvature that the velocity normal to the tangent to the line at any point is sonic. Since the linear theory permits the calculation of the local Mach numbers on the surface of the airfoil, the line which denotes the influence of the trailing edge may be calculated as

$$X = \int_0^y \sqrt{M^2 - 1} \, dy \quad (1)$$

where  $M$  is the local Mach number from linear theory. (The origin is placed at the trailing edge of the root with the positive  $X$ -axis extending downstream.) Figure 6 shows the agreement between the line denoting the foremost influence of the trailing edge so computed and the region of influence determined from the experimental pressure distribution and the liquid-film photographs discussed later. A comparison between the linear theory, revised computations, and experiment shows that the extension of the computations account for the discrepancy between the linear theory and experiment. The results of the extended computations are shown as dotted lines in figure 5.

It is interesting to note that equation (1) may be applied to the estimation of the supersonic Mach number for which the outboard sections of a swept wing of high aspect ratio may experience the same compressibility shock phenomena which, in the past, have been associated with the critical subsonic Mach number of unswept wings. In this regard, the critical supersonic Mach number for a swept wing is that Mach number for which equation (1) gives a line which lies along any constant percent chord line of the wing. For this Mach number, the component of the flow velocity perpendicular to the constant percent chord line is sonic. Mach numbers in excess of this value may result in significant changes in flow characteristics.

Examination of the data of figure 5 shows that the gradual pressure recovery predicted by the linear theory for the region influenced by the trailing edge does not occur, but, instead, a large portion of the pressure increase takes place through what seems to be a shock wave. The existence of a finite shock wave is to be expected here for the same reasons as those discussed by Riemann (reference 6) in connection with one-dimensional flows, namely, that the change of the local speed of sound in a compression wave permits the portion of the wave subject to compression to travel at a faster rate than the portion subject to expansion, thereby steepening the wave into a compression shock. No method is available which will permit the steepening of the compression regions to be calculated for this airfoil.

#### Drag

The failure of the linear theory to predict the location of the pressure minimum and the character of the compression behind the pressure minimum is significant insofar as the pressure drag of the airfoil is concerned. Figure 7 shows the spanwise variation of section-wave drag coefficient determined by integrating the pressures over the airfoil. Good agreement with theory is found on the inboard portion of the airfoil span but appreciably greater section drag coefficients occur at the outboard sections. These data indicate that the total wave drag of the airfoil is 36 percent greater than predicted by linear theory. The percentage will be somewhat greater for airfoils of higher aspect ratio with the same section and somewhat less for lower aspect ratios. The increase in drag over that predicted by linear theory will be less for smaller thickness ratios.

#### Boundary-Layer Studies

Use was made of the liquid-film technique, which has been discussed fully in reference 5, to investigate the character of the boundary-layer flow. This method of visualizing the boundary-layer flow makes use of the fact that the rate of evaporation of a volatile liquid from the surface of the airfoil is a function of the surface shearing stress. Since the shear in the region of the turbulent boundary layer is, in general, much higher than for the laminar boundary layer, the surface of the airfoil behind the point of transition from laminar to turbulent flow in the boundary layer will become dry before the region ahead of the transition point, the areas subject to laminar and turbulent flow thereby being defined.

Figure 8 shows photographs of the liquid film at three test Reynolds numbers during tunnel operation.<sup>1</sup> The airfoil shown on the top photograph has been exposed to the air stream a shorter time than the one at the bottom. The results of these studies show that, at the lowest Reynolds number, the surface shear is relatively small over the airfoil surface except near the leading edge where high laminar shear exists. The pressure-distribution test discussed previously showed that laminar separation occurred at this Reynolds number so that it is to be expected that the surface shear would be small. Usually, the occurrence of laminar separation results in the formation of a ridge of fluid at the separation point. The present tests do not show this phenomenon, possibly because the surface tension of the liquid film is great enough, in comparison with the viscous forces of the air stream (at the necessary low test pressure), to prevent the ridge from being formed.

At the higher Reynolds numbers, the liquid film has completely evaporated in the region just ahead of the trailing edge after a short period of exposure of the airfoil surface to the stream. The liquid-film studies of figure 8 show that transition to turbulent flow is occurring on the airfoil ahead of the location of the experimental minimum pressure point shown by the dashed line.<sup>2</sup> In this case, the boundary layer has sufficient energy to enable it to flow some distance against the adverse pressure gradient over the rear of the airfoil so that the separation, now turbulent, is confined to the region near the trailing edge indicated by the extreme cross flow.

The liquid-film photographs at the highest Reynolds numbers show that the location of the transition point moves forward rapidly with increasing Reynolds number in spite of the fact that the pressure gradient is favorable to laminar flow, much more rapidly, in fact, than for a corresponding Reynolds number range at subsonic Mach numbers. Whether this is due to the turbulence of the wind-tunnel air stream or other outside causes, or whether this is an essential characteristic of the boundary layer at supersonic speed, is not known. The surface of the model was very smooth and free from waves so that no surface roughness effects were present. Further research directed toward investigation of these boundary-layer characteristics is indicated, including the effect of curvature of the surface.

---

<sup>1</sup>The photographs shown have been retouched to preserve the definition of the liquid-film pattern usually lost in the reproduction process.

<sup>2</sup>The dashed line was determined from faired pressure-distribution data and agrees well with the location of the pressure minimum shown by the sudden bending of liquid-film streamers.

---

CONFIDENTIAL  
CONCLUDING REMARKS

The results of the experimental investigation show that the distribution of pressure at zero lift over the surface of an airfoil swept behind the Mach cone can be calculated with reasonable accuracy from thin airfoil theory except in the regions influenced by the subsonic trailing edge and the tip. The deviation of theory from experiment in these regions is a function of the thickness-chord ratio of the airfoil and is manifest in the following:

1. The region of influence of the subsonic trailing edge is shifted rearward. This effect can be calculated from consideration of the local Mach number on the airfoil surface.

2. The pressure recovery behind the pressure minimum is greater than predicted by theory and, although the data are not conclusive, appears to take place, in part, through a shock wave.

The net result of these effects is an increase in the pressure drag coefficient over that given by linear theory.

Studies of the boundary-layer flow show that transition from laminar to turbulent flow occurred on the airfoil at Reynolds numbers greater than  $1 \times 10^6$ . As the Reynolds number was increased to  $3.25 \times 10^6$ , the location of the transition point moved rapidly forward, even though the pressure gradient is favorable to laminar flow.

Ames Aeronautical Laboratory,  
National Advisory Committee for Aeronautics,  
Moffett Field, Calif.

## REFERENCES

1. Ackeret, J.; Air Forces on Airfoils Moving Faster Than Sound. NACA TM No. 317, 1925.
2. Jones, Robert T.: Thin Oblique Airfoils at Supersonic Speed. NACA TN No. 1107, 1946.
3. Puckett, Allen E.: Supersonic Wave Drag of Thin Airfoils. Jour. Aero. Sci., vol. 13, no. 9, Sept. 1946, pp. 475-484.

CONFIDENTIAL

4. Van Dyke, Milton D.: Aerodynamic Characteristics Including Scale Effect of Several Wings and Bodies Alone and in Combination at a Mach Number of 1.53. NACA RM No. A6K22, 1946.
5. Vincenti, Walter G., Nielsen, Jack N., and Matteson, Frederick H.: Investigation of Wing Characteristics at a Mach Number of 1.53. I - Triangular Wings of Aspect Ratio 2. NACA RM No. A7I10, 1947.
6. Riemann, B.: Note on the Propagation of Plane Air Waves of Finite Oscillation Amplitude. Abhandlungen der Koniglichen Gesellschaft der Wissenschaften zu Gottingen. 1858-1859, v. 8, pp. 43-65.

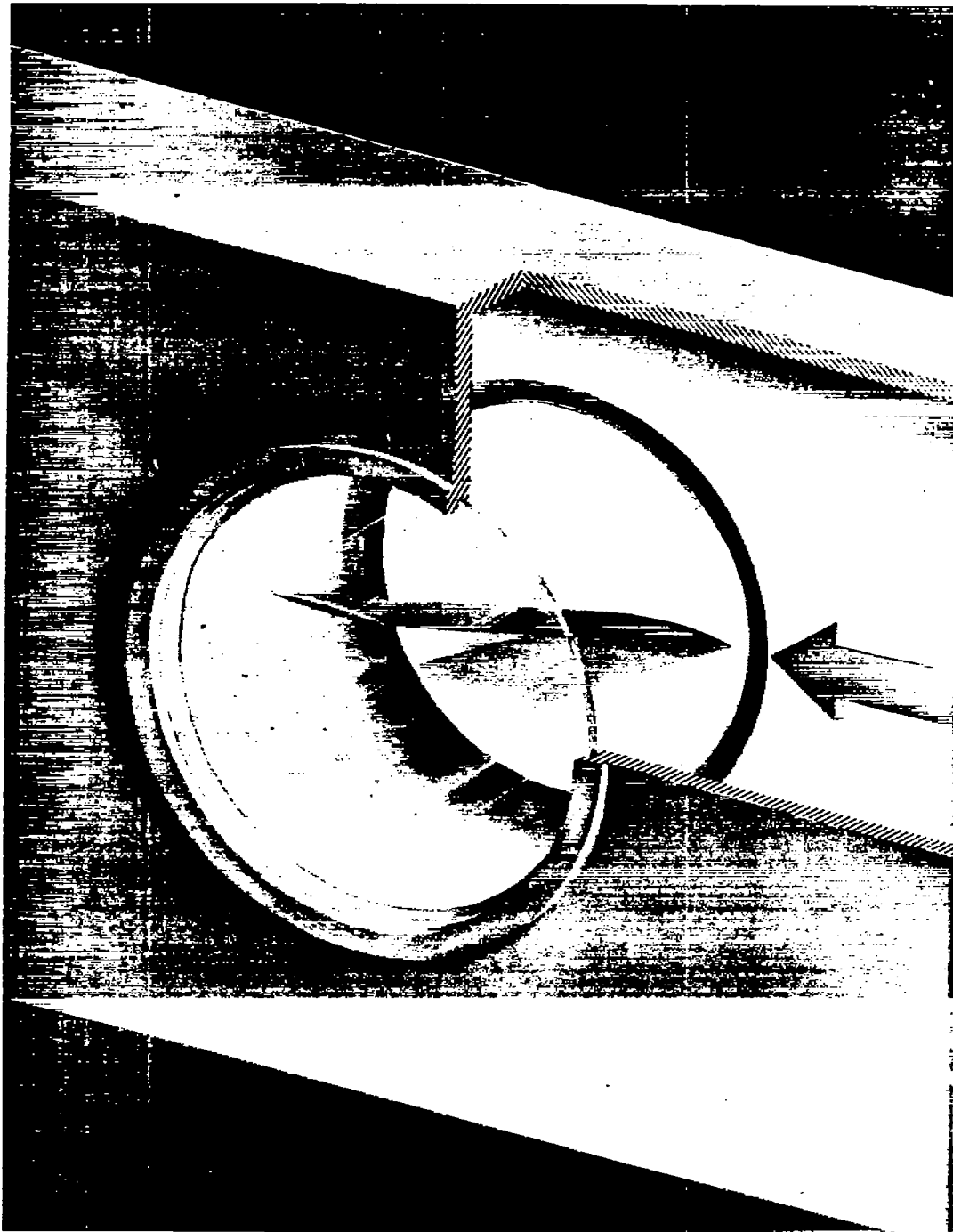


Figure 1.- Sketch of airfoil mounted for test.

NACA  
A-12342



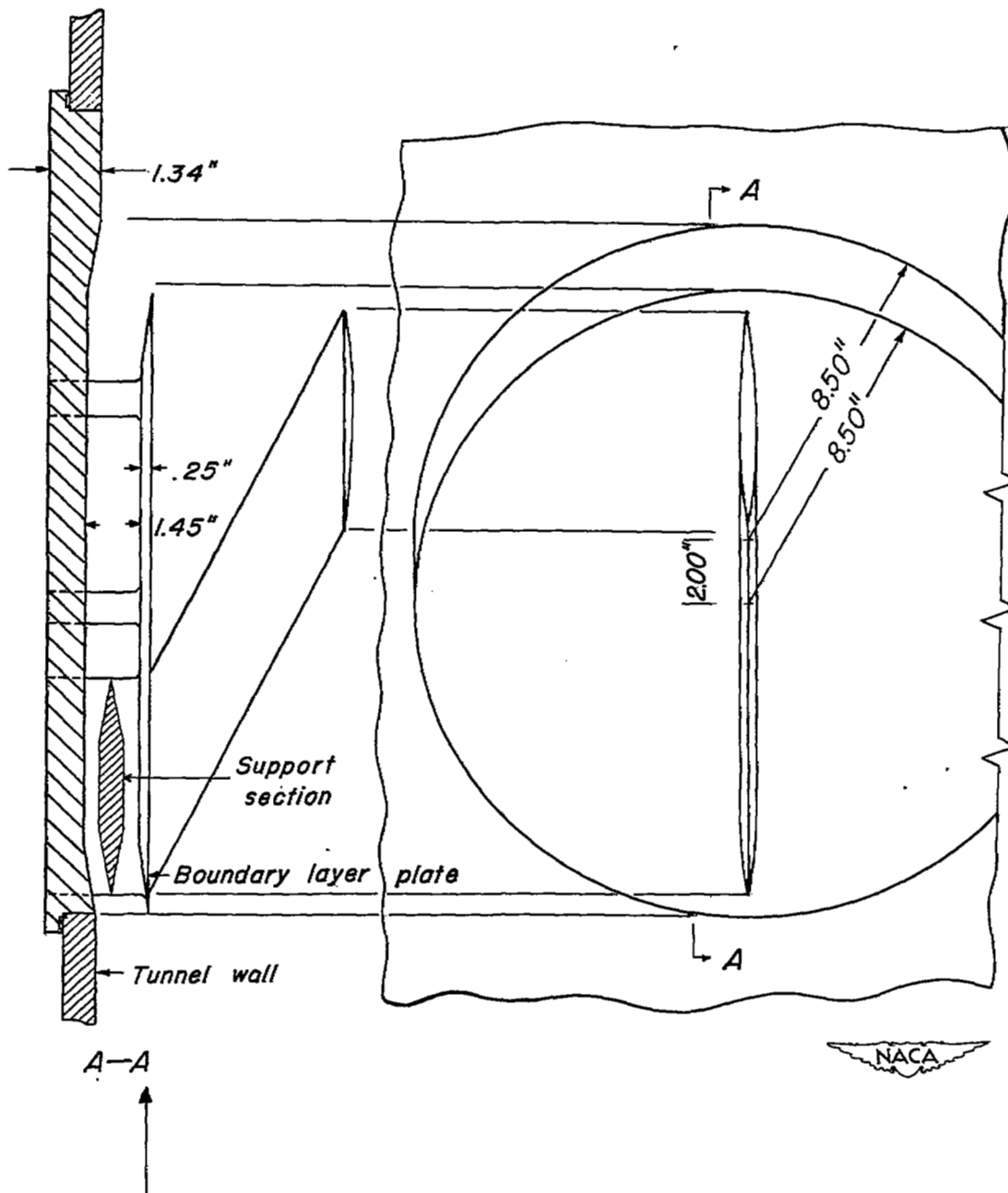


Figure 2.— Sketch of model support system

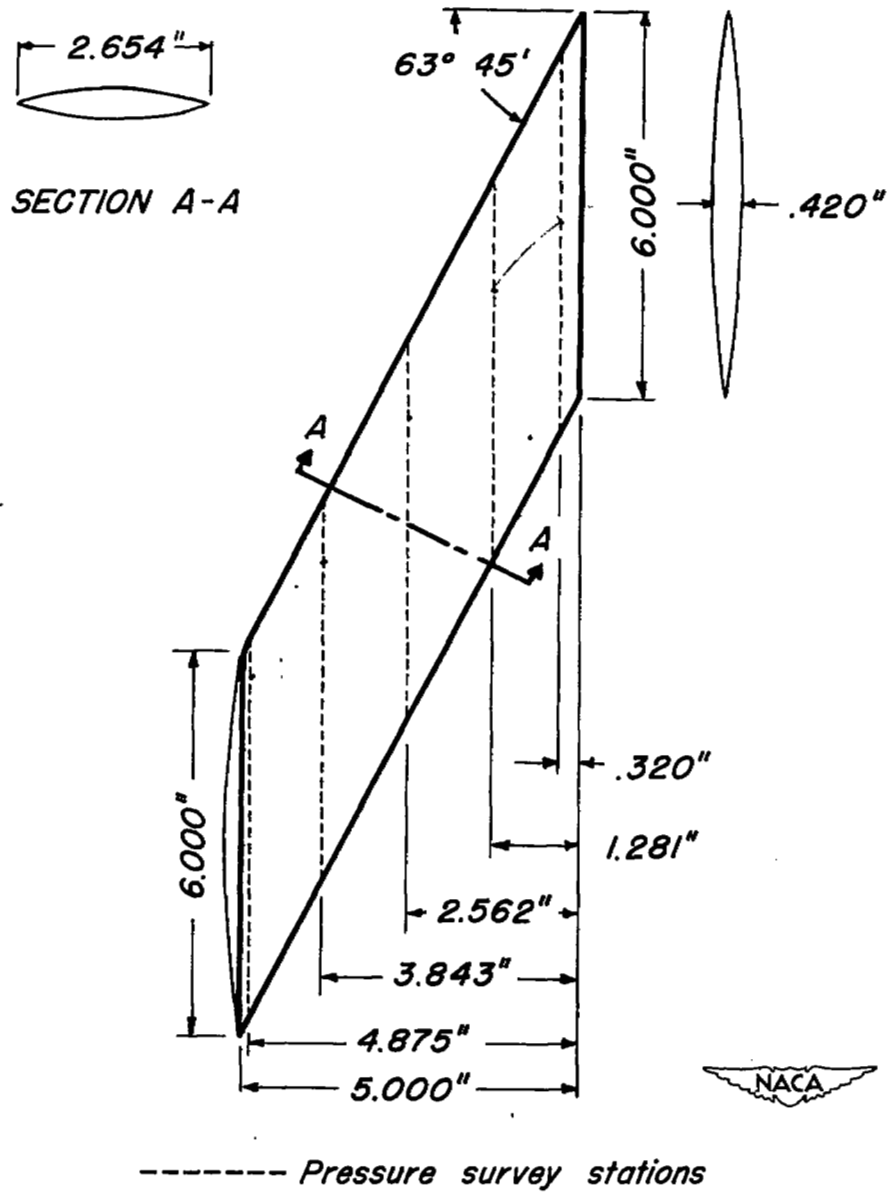
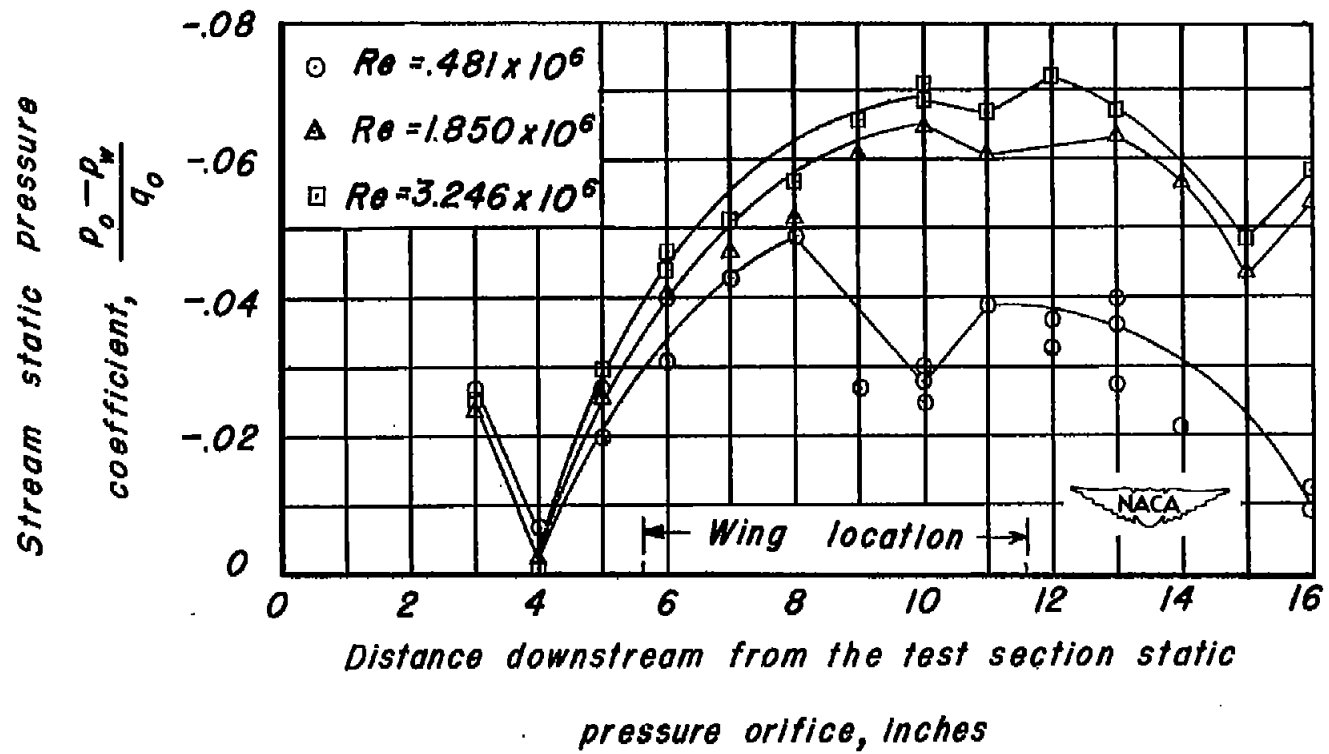
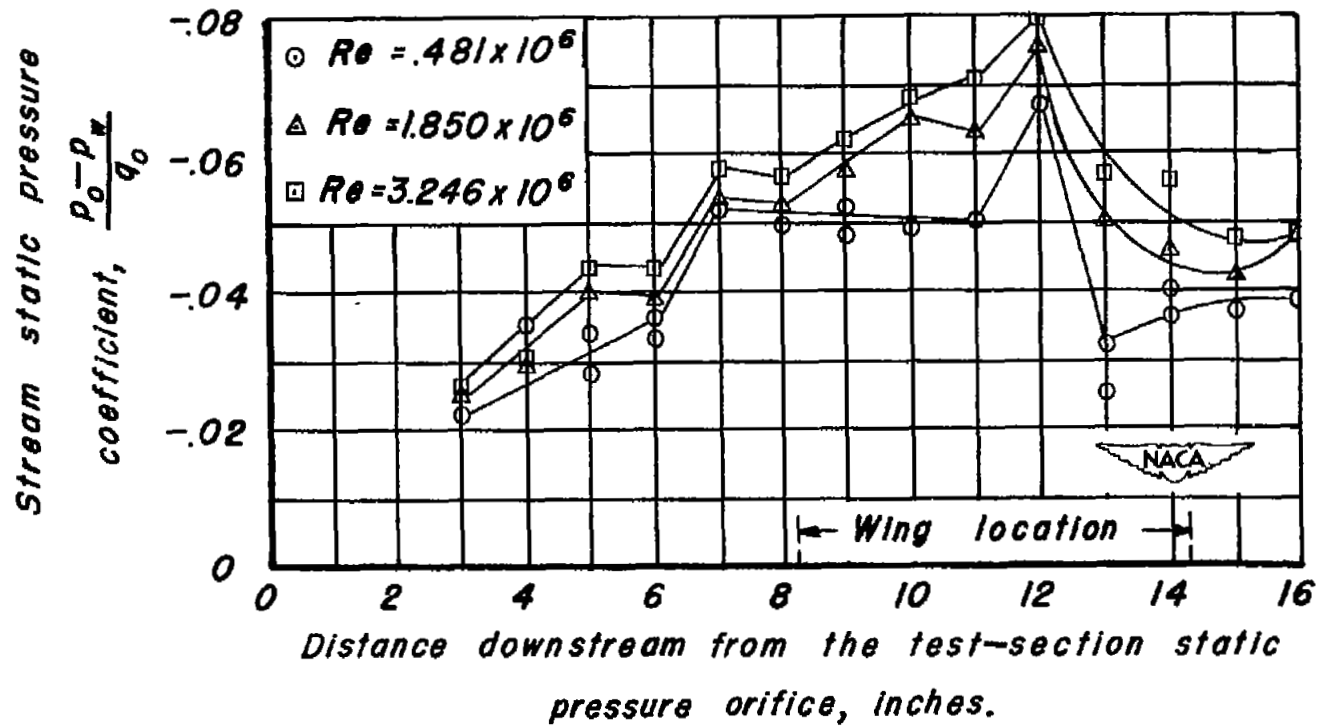


Figure 3.— Dimensional sketch of model showing pressure survey stations



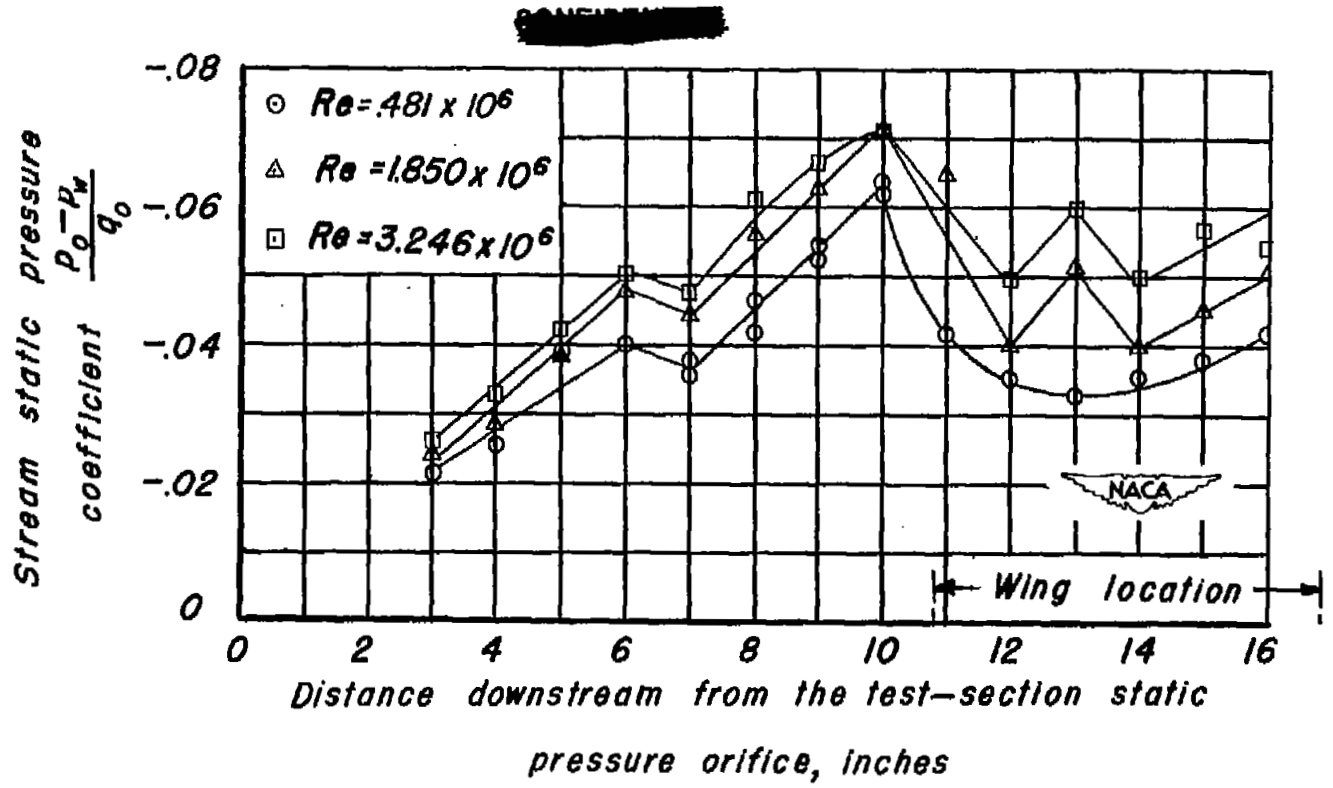
(a) 25 - percent of model span from root.

Figure 4.— Axial static pressure variation in wind-tunnel stream.



(b) 50-percent model span from root.

Figure 4. - Continued.

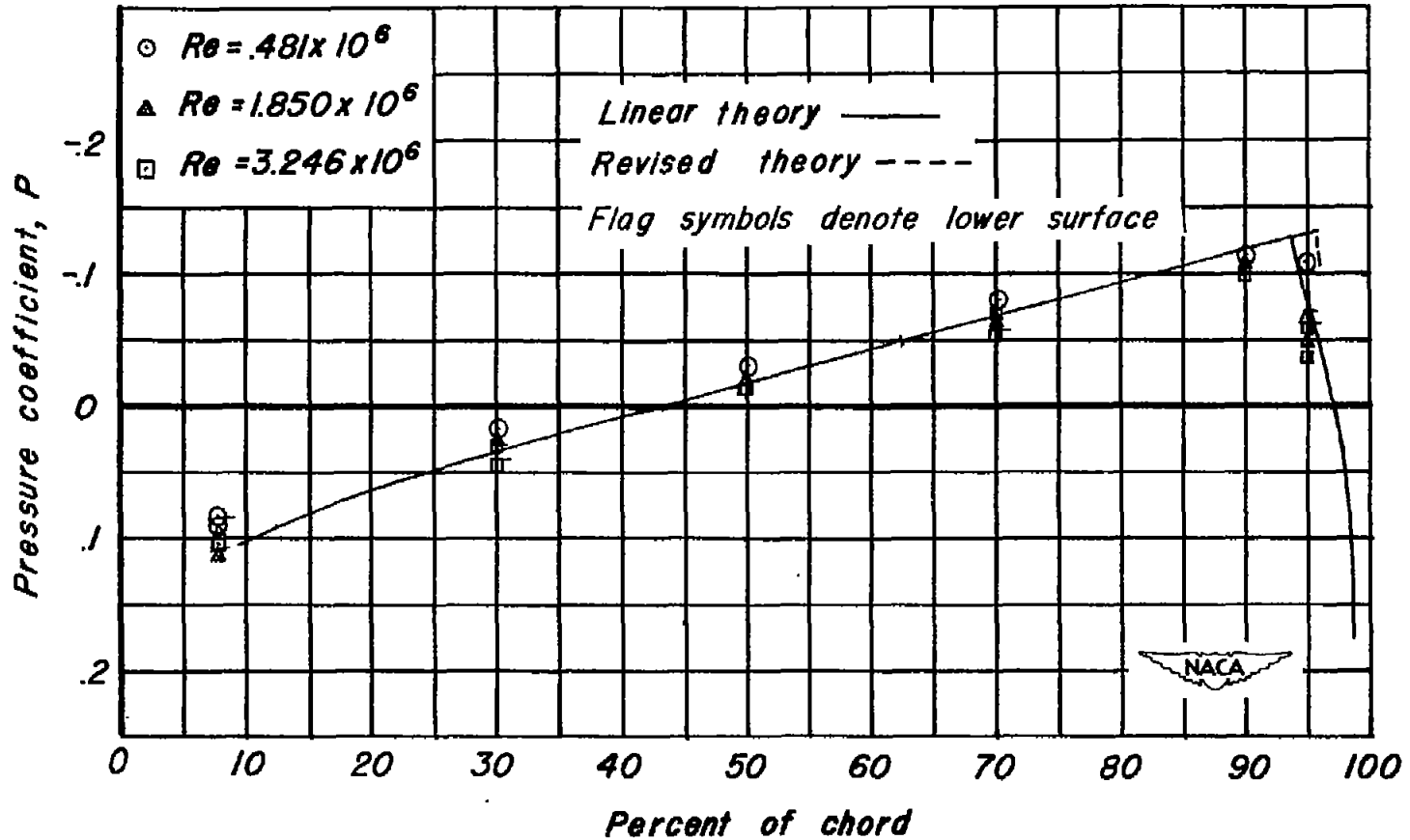


(c) 75— percent model span from root.

Figure 4.— Concluded.

**CONFIDENTIAL**

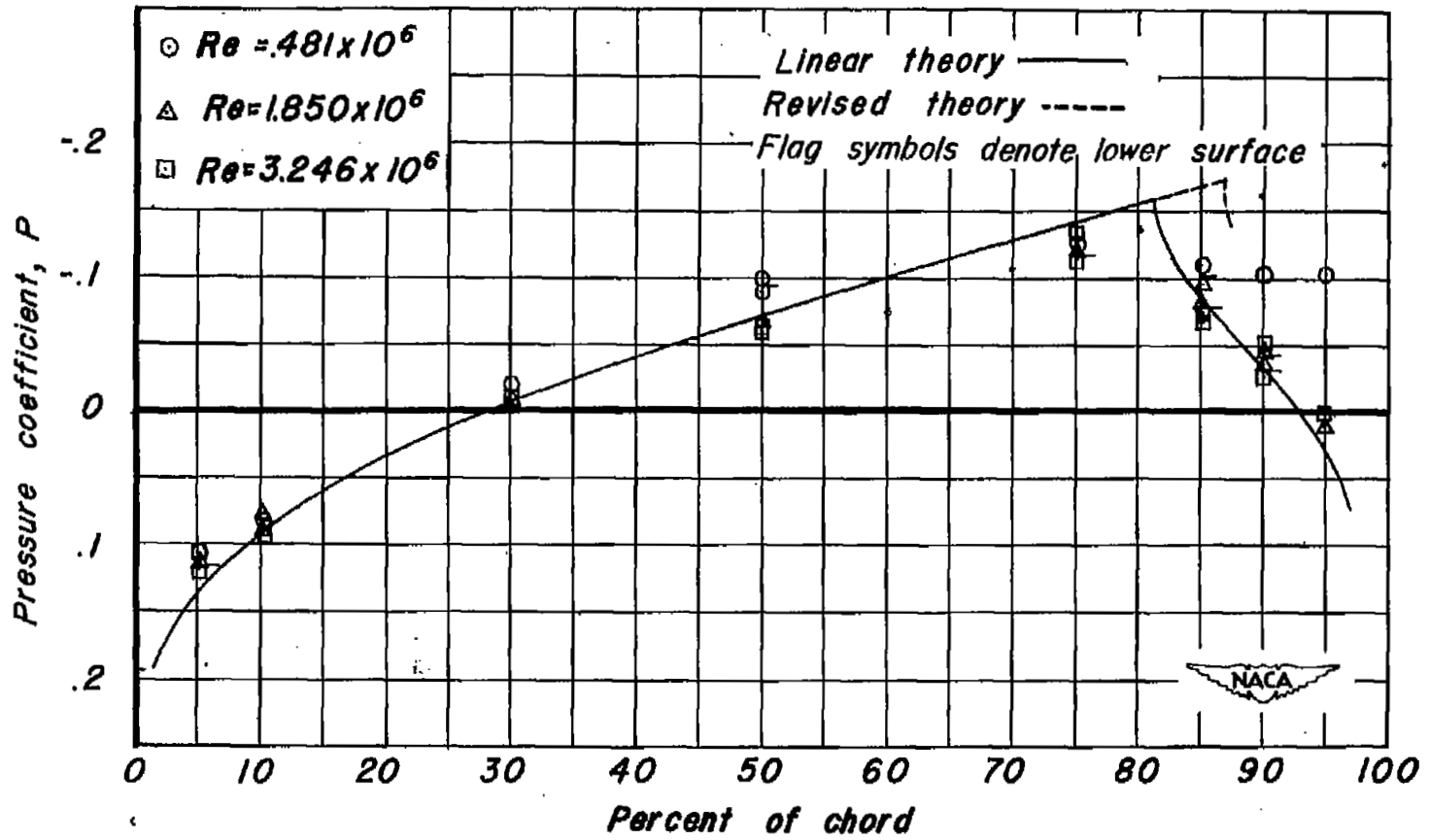
~~CONFIDENTIAL~~



(a) Station 6.4-percent semispan.

Figure 5.— Chordwise pressure distribution over swept-back airfoil at zero lift.

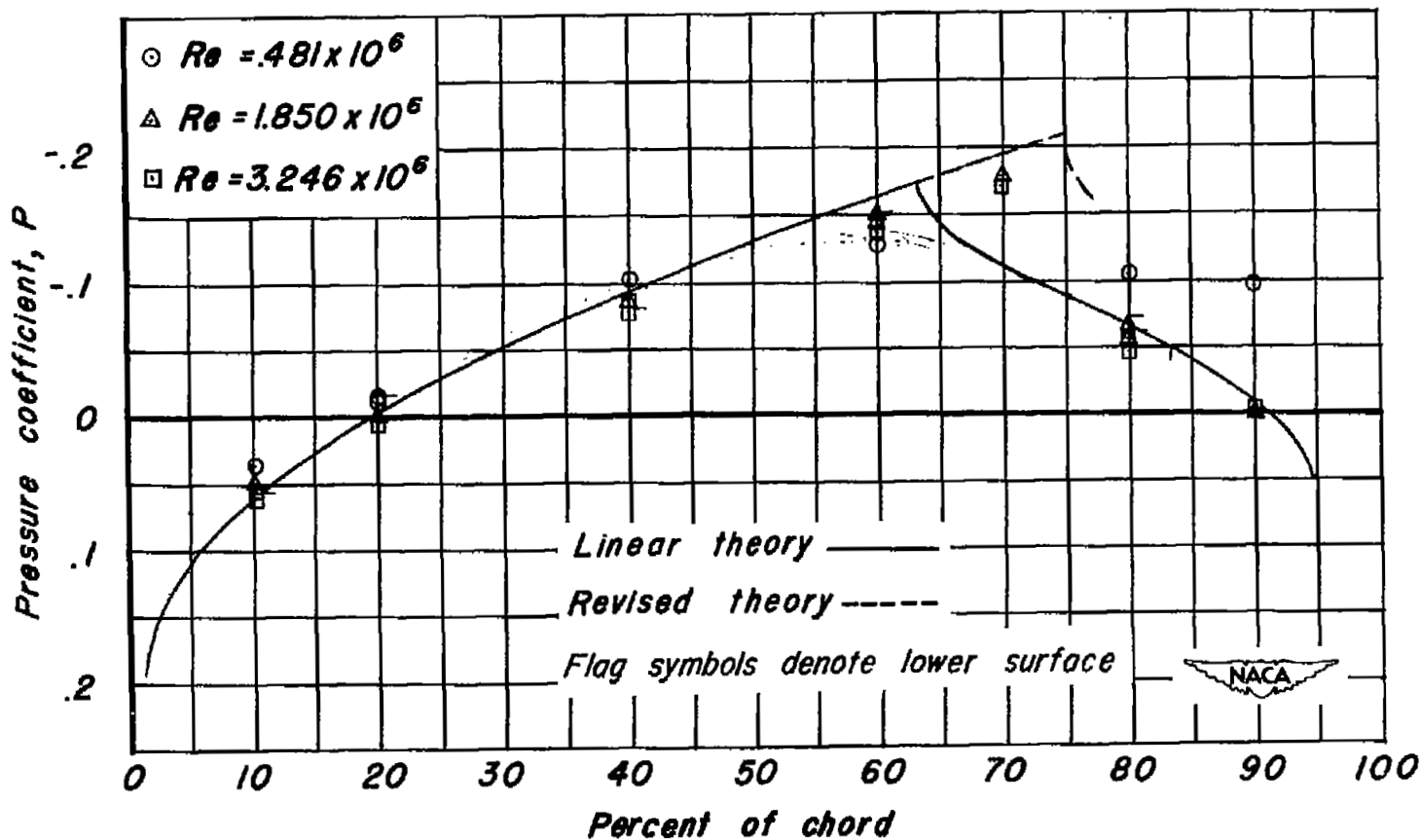
~~CONFIDENTIAL~~



(b) Station 25.6-percent semispan.

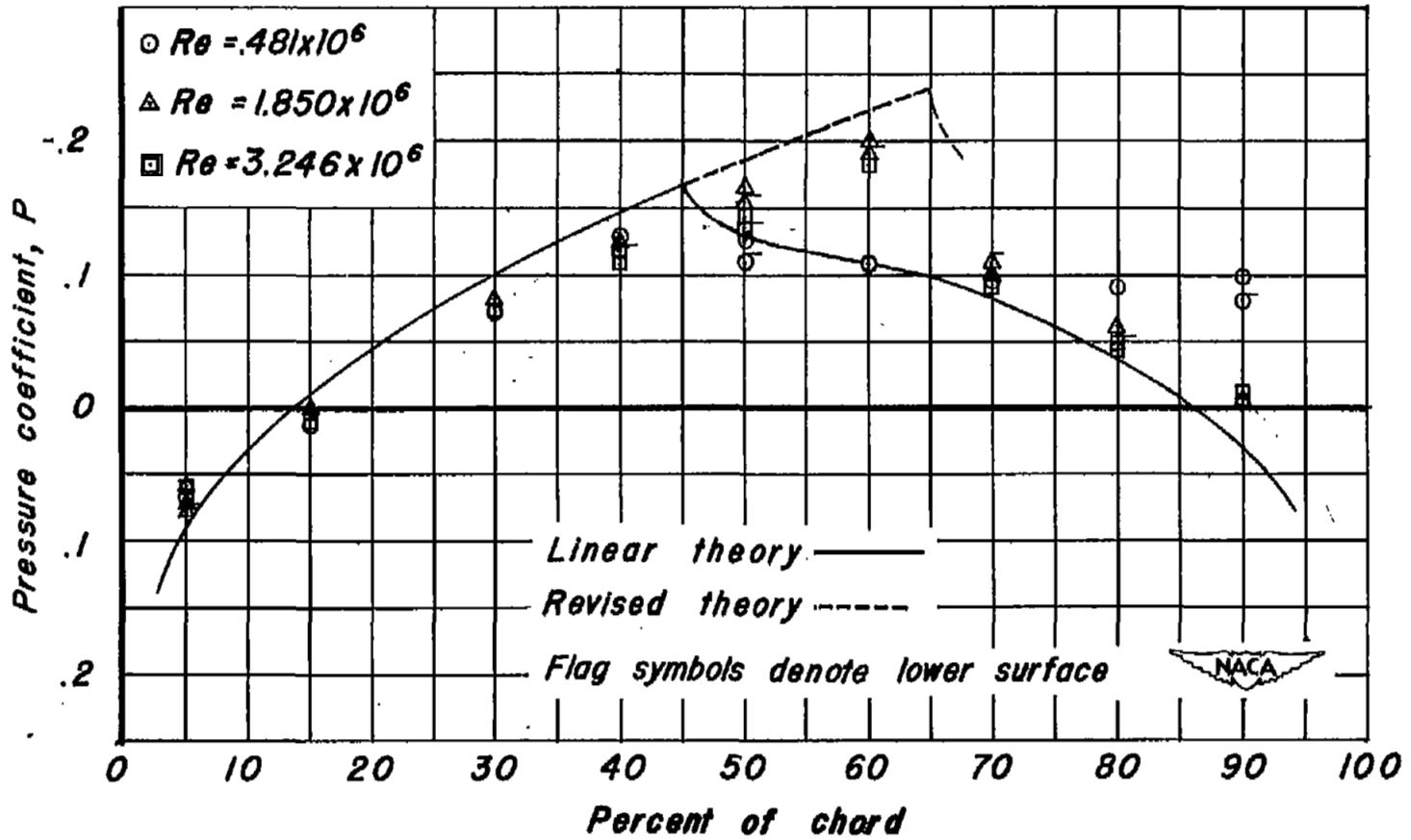
Figure 5.- Continued.

CONFIDENTIAL



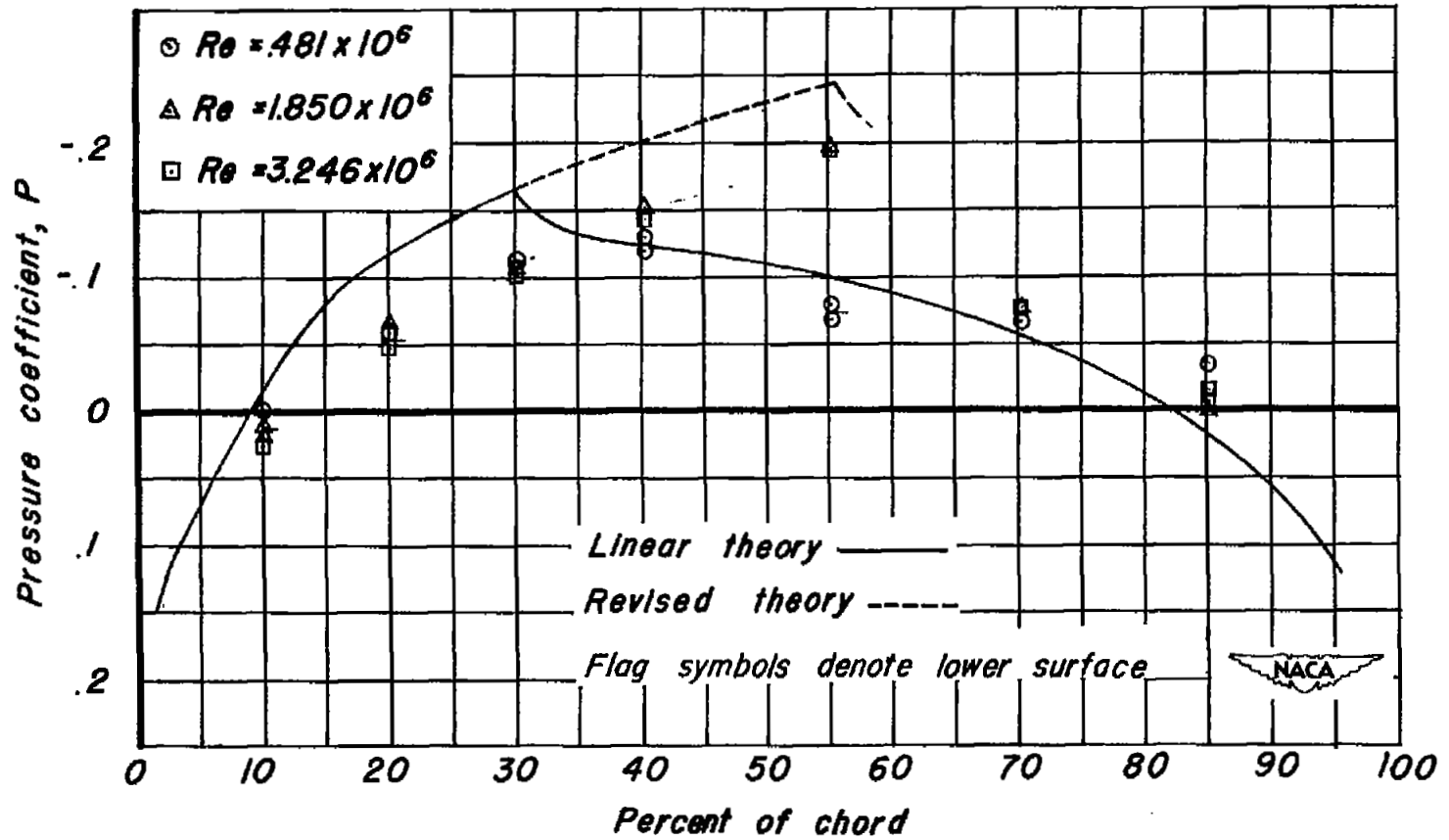
(c) 51.24-percent semi-span.

Figure 5.- Continued.



(d) 76.86-percent semispan.

Figure 5.—Continued.



(e) 97.5-percent semispan.

Figure 5.— Concluded.

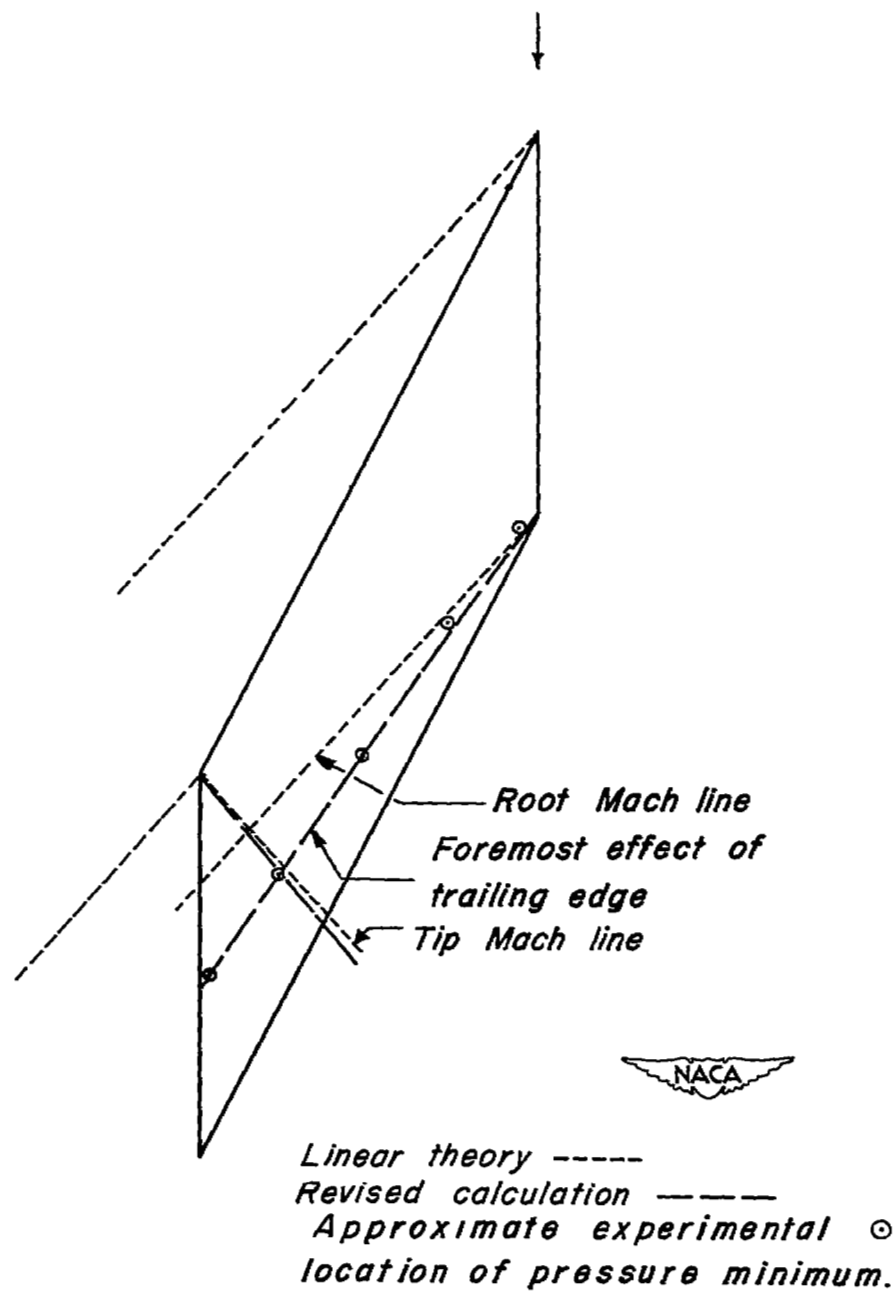


Figure 6.— Comparison of region of influence of trailing edge and tip from experiment, linear theory, and revised linear theory

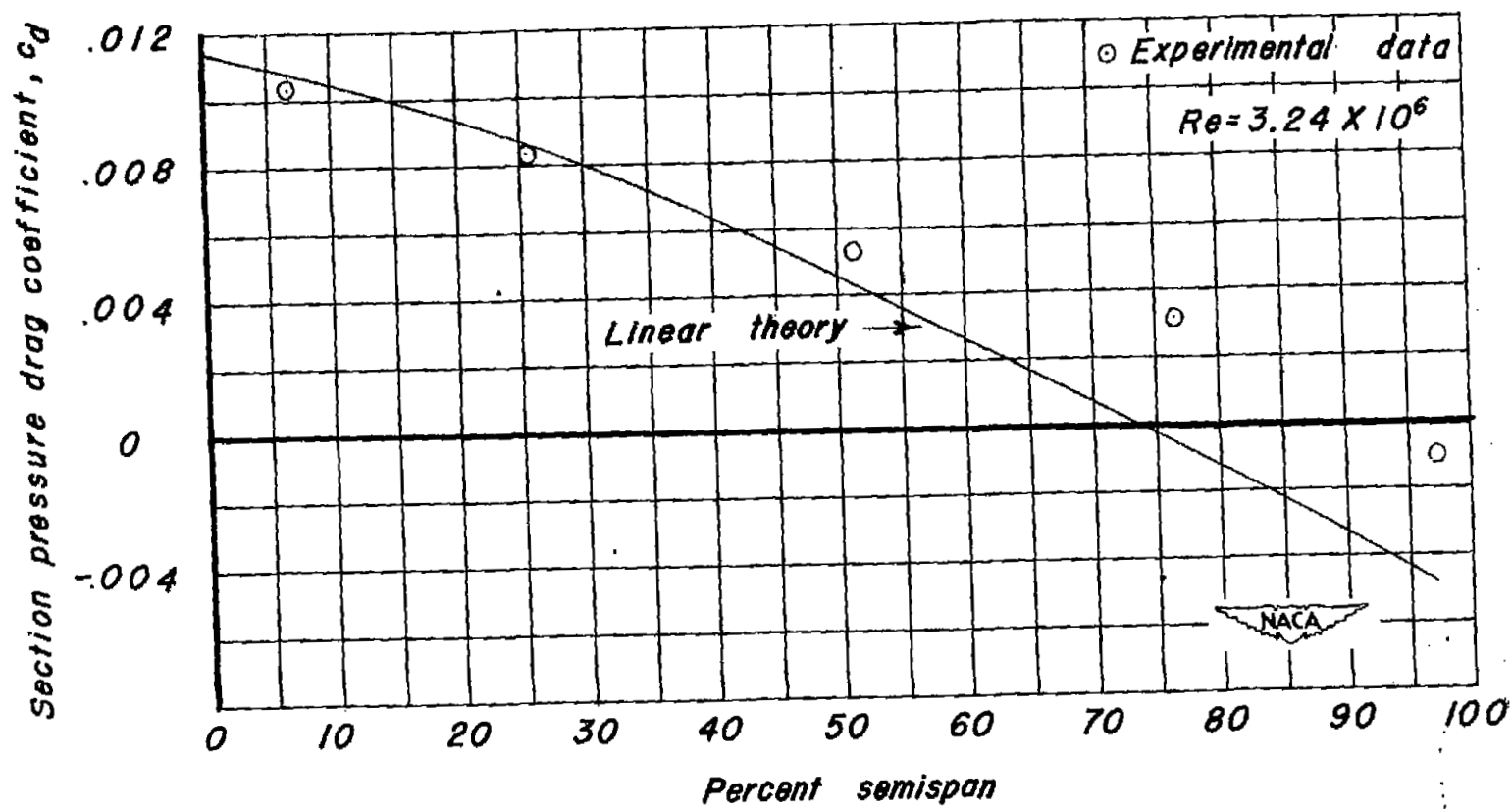
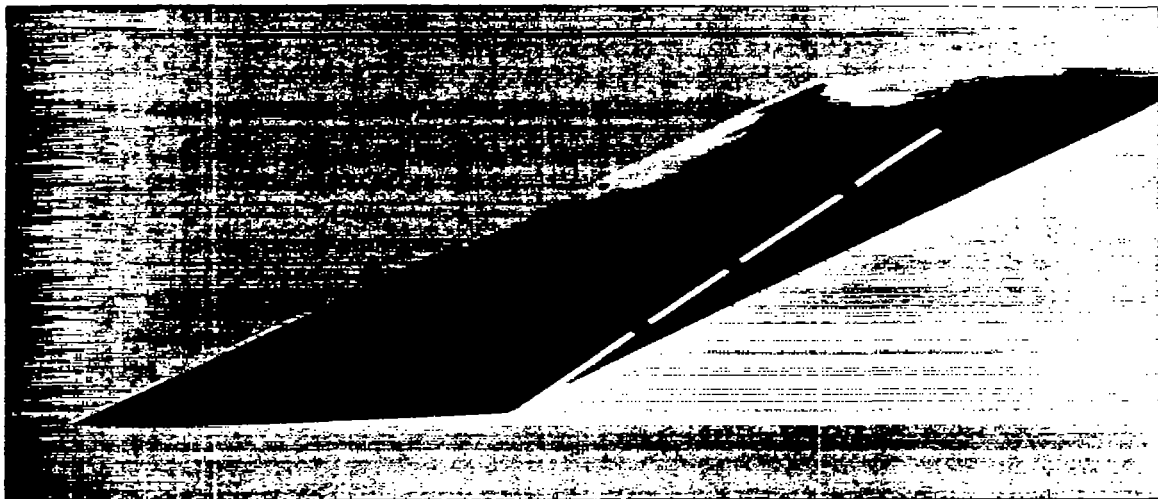
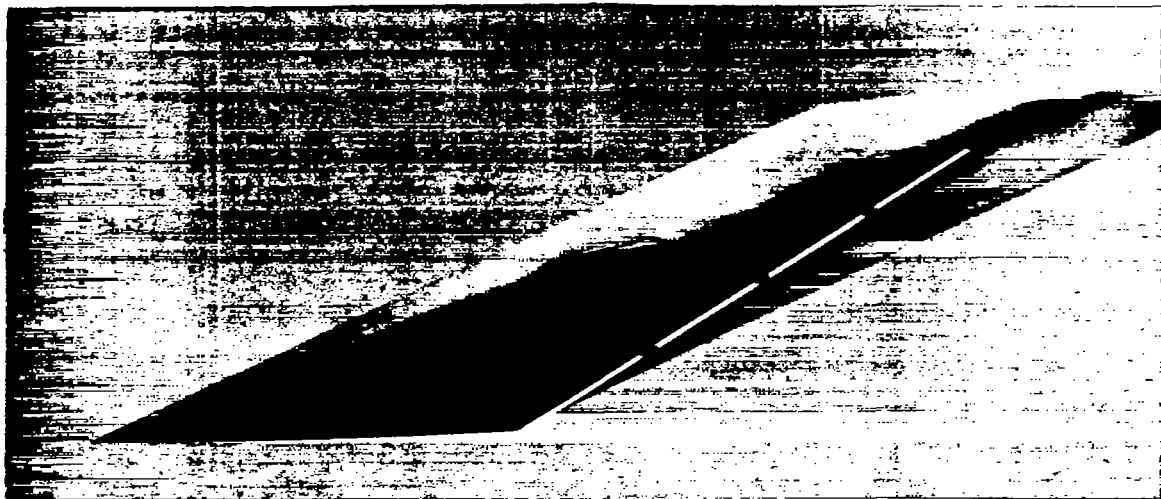


Figure 7.—Spanwise variation of section pressure drag coefficient for the swept-back airfoil.



(a) Reynolds number =  $0.905 \times 10^6$ . Exposed to air stream for short period of time.



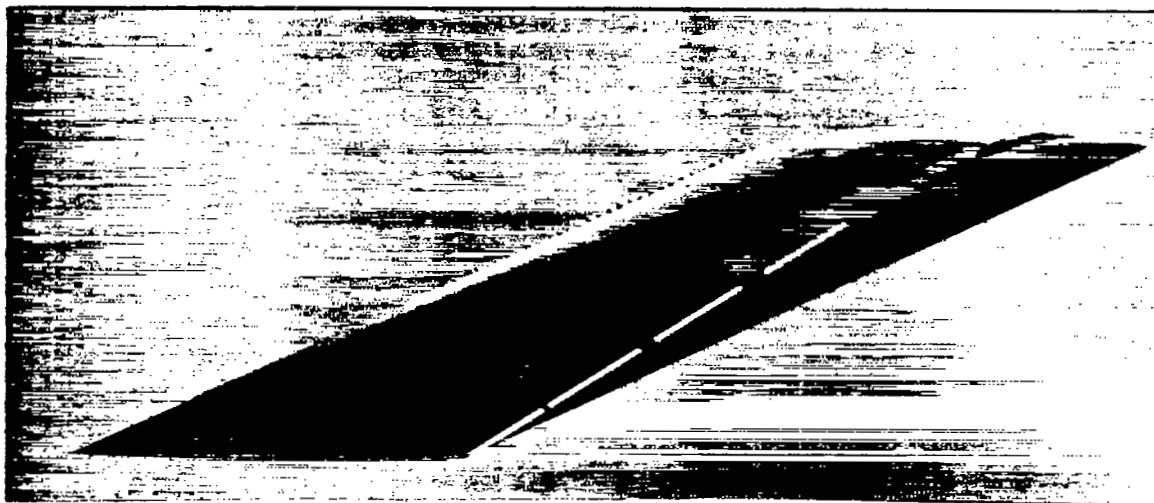
(b) Reynolds number =  $0.905 \times 10^6$ . Exposed to air stream for long period of time.

The NACA logo, consisting of the letters "NACA" inside a stylized wing shape.

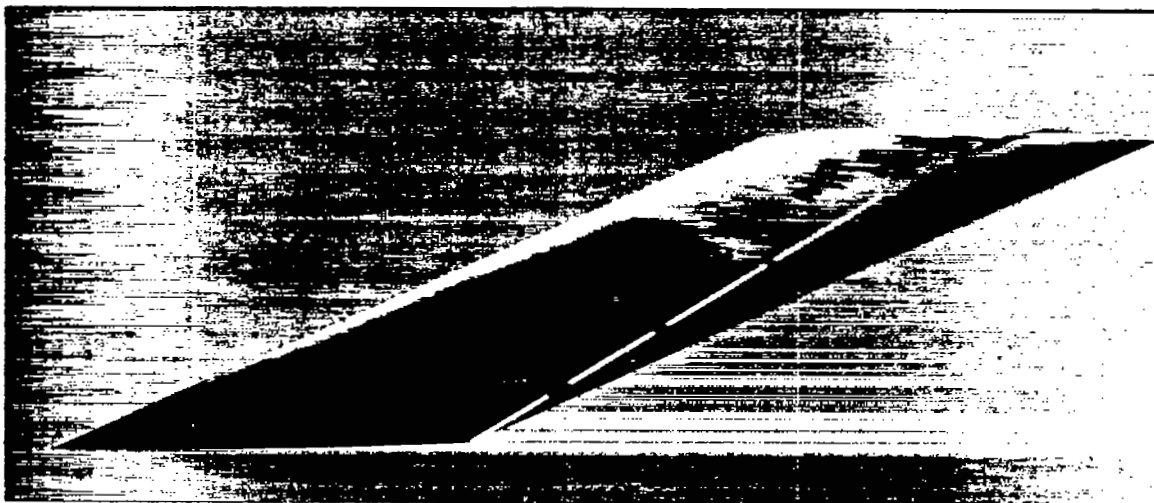
A-12429

Figure 8.— Photographs of liquid film.  $M = 1.53$ .





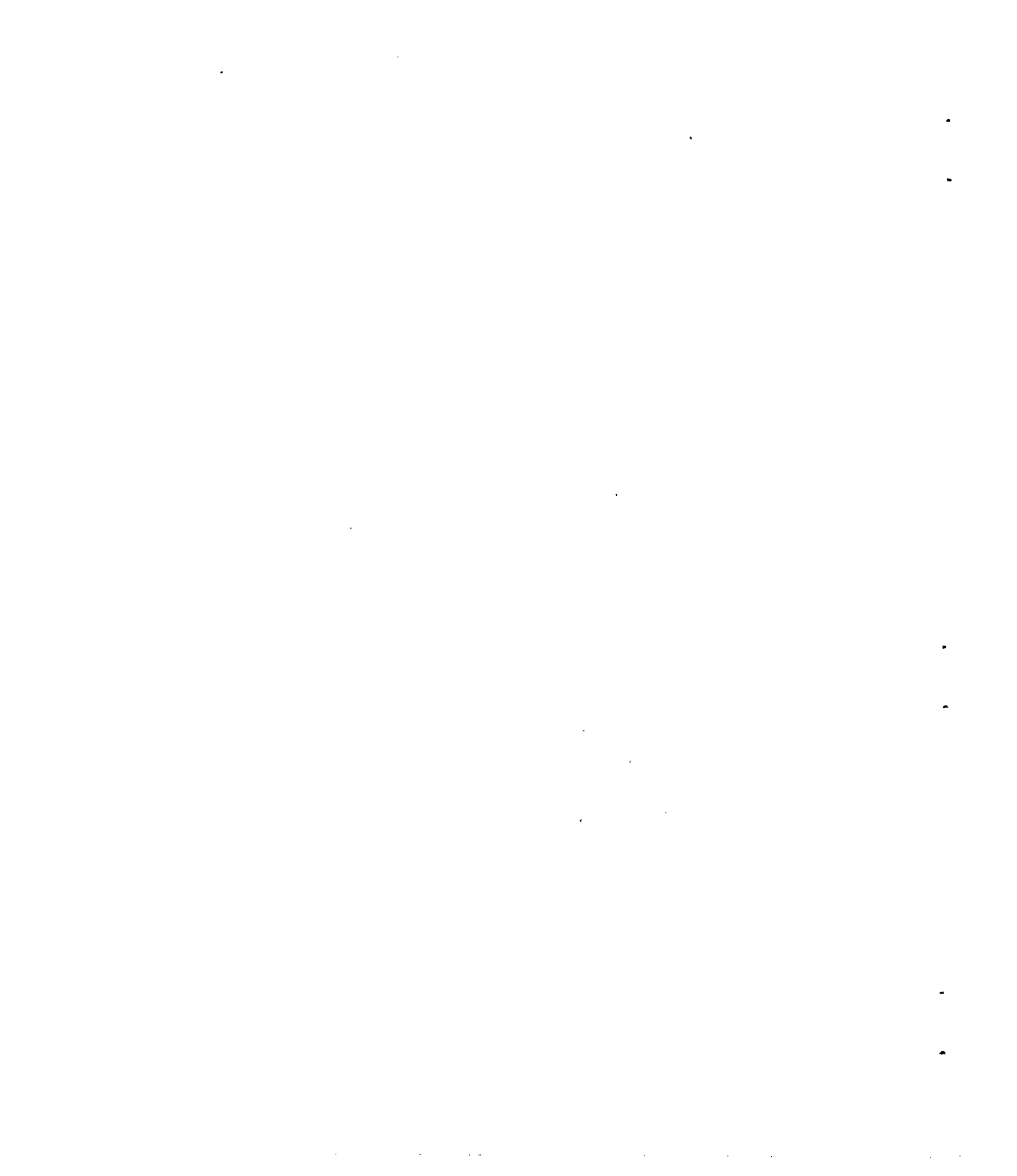
(c) Reynolds number =  $1.809 \times 10^6$ . Exposed to air stream for short period of time.

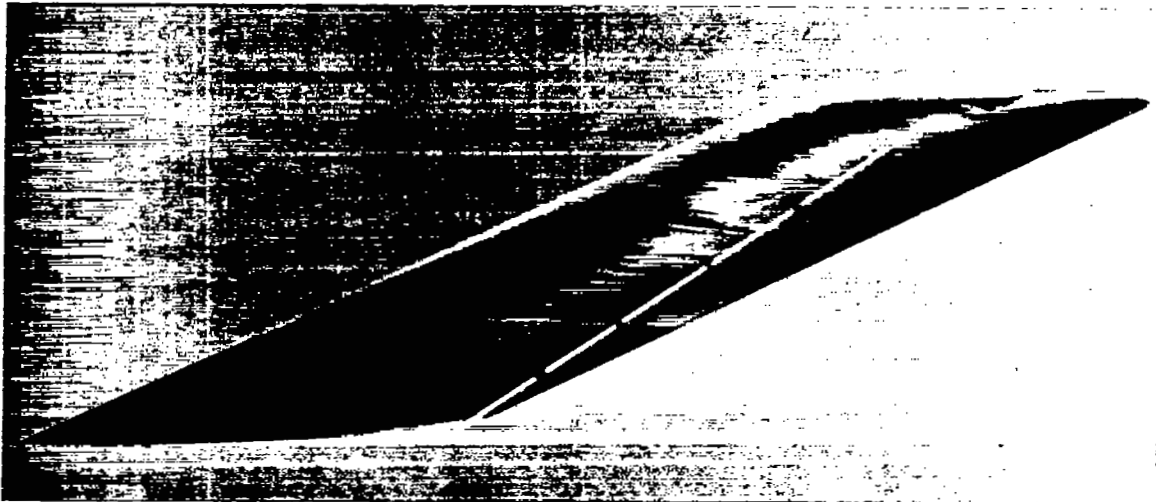


(d) Reynolds number =  $1.809 \times 10^6$ . Exposed to air stream for long period of time.

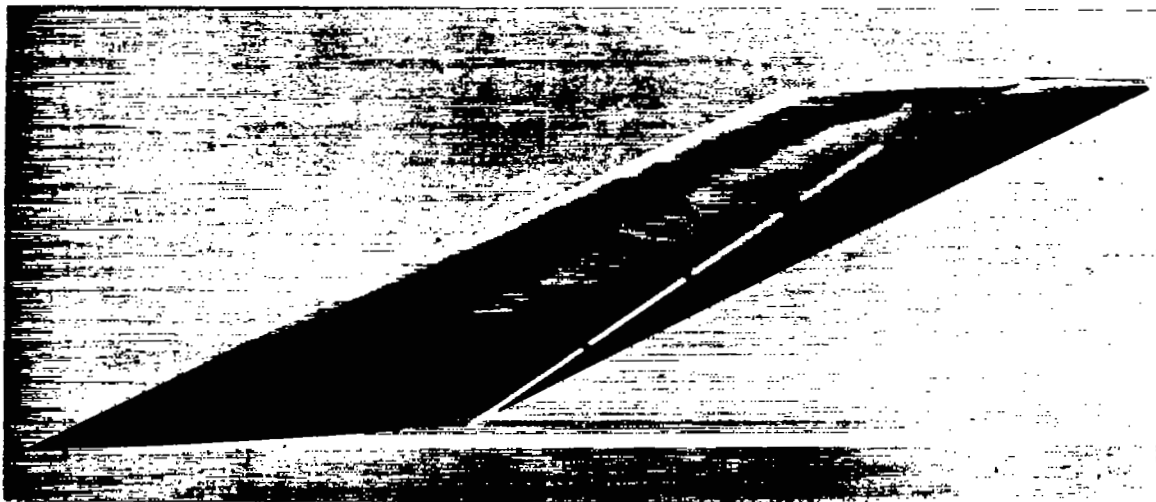
NACA  
A-12430

Figure 8.- Continued.





(e) Reynolds number =  $3.166 \times 10^6$ . Exposed to air stream for short period of time.



(f) Reynolds number =  $3.166 \times 10^6$ . Exposed to air stream for long period of time.

Figure 8.— Concluded.



LANGLEY RESEARCH CENTER

3 1176 01328 6365